Structural and magnetic properties of epitaxially grown MnAs films on GaAs(110)

D. Kolovos-Vellianitis,[a] C. Herrmann, L. Däweritz, and K. H. Ploog
Paul-Drude-Institut für Festkörperelektronik, Hausvogteiplatz 5-7, D-10117 Berlin, Germany

(Received 15 February 2005; accepted 8 July 2005; published online 23 August 2005)

MnAs films were grown by molecular beam epitaxy (MBE) on GaAs(110) substrates, since this orientation was recently identified as promising for the increase of spin lifetimes in semiconductor heterojunctions, which is of interest in spin injection experiments. A single epitaxial orientation was revealed for the MnAs films which consist of both the ferromagnetic, hexagonal α-MnAs and the paramagnetic, orthorhombic β-MnAs phase at room temperature. This phase coexistence could be imaged as a well ordered stripe pattern, whose periodicity depends on the film thickness. The study of the ferromagnetic properties shows a strong influence of the film thickness on the measured coercive fields and saturation magnetizations. © *2005 American Institute of Physics*. [DOI: 10.1063/1.2035328]

The prospect of utilizing both the electron charge and spin in future optoelectronic devices requires the development of materials, which combine ferromagnetic and semiconducting properties.[1] In particular, the injection of spin polarized carriers into nonmagnetic materials has become a major challenge in the past few years, since logical operation could be implemented by manipulating the two allowed spin states.[2] The successful heteroepitaxial growth of MnAs on (001), (111), and (113) oriented GaAs substrates[3–8] has already established controlled systems in terms of their structural and magnetic properties. Furthermore, the coexistence of α-MnAs and β-MnAs in the epitaxial films and the dependence of the magnetic properties on film thickness have been well described in recent works.[4,9–11] Finally, the Curie temperature (T_C) above room temperature (RT) and the relatively small coercive field (50 Oe) of MnAs have led to investigations about the spin-injection efficiency from this ferromagnetic metal into GaAs(001), which amounts to about 6% at 80 K.[12]

A very important factor affecting the detection of the spin-injection efficiency is the relaxation time of the electron spin τ_S, which must be sufficiently long for spin memory devices or spin quantum computers. Spin relaxation in GaAs(001) quantum wells (QWs) have been widely studied and revealed that the D'yakonov-Perel' (DP) mechanism plays a dominant role at higher temperatures.[13] Recent studies have reported that τ_S in both undoped and well-doped GaAs(110) QWs is increased from the picosecond to the nanosecond range at RT.[14] The temperature dependence of τ_S supports the suggestion that electron-hole interaction governs the spin relaxation in (110) QWs rather than the DP or the Elliott–Yafet (EY) mechanism.[15]

The above observations motivated this study, which presents results about the growth, structural and magnetic properties of MnAs on GaAs(110) substrates. Reflection high-energy electron diffraction (RHEED) was applied to monitor the growth of the MnAs films and to determine its orientation on the GaAs(110) substrate. X-ray diffraction (XRD) and atomic force microscopy (AFM) measurements were also performed for further structural analysis, whereby superconducting quantum interference device (SQUID) magnetometry was used in order to characterize the magnetic properties on a macroscopic scale.

The MnAs films were grown on singular *n*-type GaAs(110) substrates by standard solid-source MBE with an As valve cracker cell. After deposition of a high-temperature GaAs buffer layer of 450 nm thickness at $T \approx 600$ °C, the templates were transferred to the MnAs growth chamber. After the oxide desorption, the sample was cooled down to $T = 250$ °C where a (1×1) RHEED pattern was observed. MnAs was then grown at a growth rate of 20 nm h^{-1} with an As_4/Mn beam equivalent pressure (BEP) ratio of 200 by codeposition of Mn and As, while the thickness of the MnAs films was varied between 24 nm and 200 nm. The Mn flux was calibrated by RHEED-intensity oscillations and by cross-sectional thickness measurements using scanning electron microscopy (SEM). After growth the substrate temperature was reduced to RT with a rate of 1 °C/min.

The As–Mn phase diagram[16] reveals the existence of several MnAs phases with different structures. The paramagnetic NiAs-type γ-MnAs is stable at typical film growth temperatures (250 °C) with a phase transition towards to the paramagnetic, orthorhombic MnP-type β-MnAs occurring at 125 °C. A further phase transition of first order takes place at $T \approx 40$ °C and leads to the ferromagnetic α-MnAs, which shows again the hexagonal NiAs structure. The (110) surface of GaAs is composed of zigzag ridges of Ga and As running parallel to the $[\bar{1}10]$ direction. The relaxed surface shows atomic displacements in the surface and first subsurface layers, whereas the distances between the lattice planes along the $[\bar{1}10]$ and the [001] direction are 5.654 and 3.998 Å, respectively.[17]

The epitaxial orientation of MnAs on the GaAs(110) substrate was determined by RHEED during growth and by post-growth XRD measurements. Figures 1(a) and 1(b) show the RHEED patterns when the electron beam is directed along the [001] and $[\bar{1}10]$ direction of the GaAs(110) substrate, respectively, during the first stages of the MnAs formation. The RHEED patterns remain streaky throughout nucleation and growth, indicating 2D-growth while the

[a]Author to whom correspondence should be addressed; electronic mail: kolovos@pdi-berlin.de

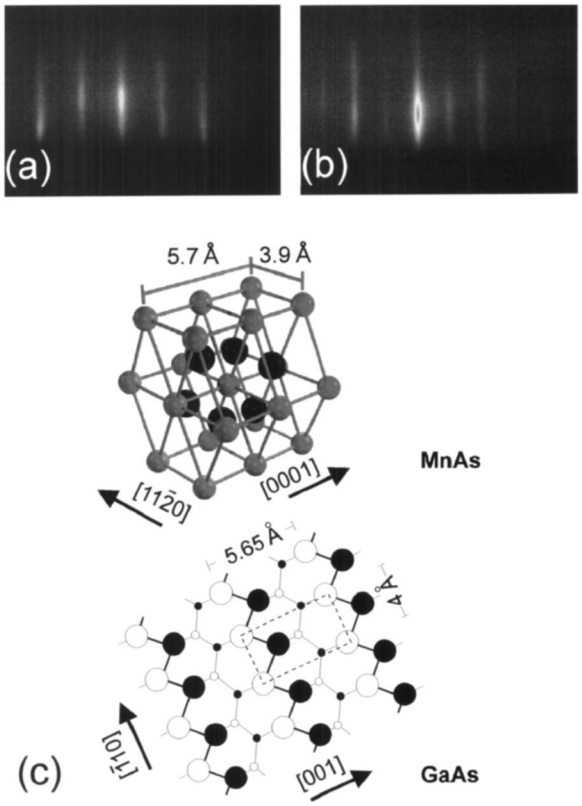

FIG. 1. (a), (b) RHEED patterns taken in the [11$\bar{2}$0] and [0001] azimuths, respectively, of the MnAs($\bar{1}$100) surface during growth, film thickness of 65 nm. (c) Epitaxial relationship between the hexagonal MnAs bulk lattice and the GaAs(110) surface (As- and Ga atoms are drafted by solid and open circles, respectively, whereby small circles indicate deeper atomic layers).

sharpness of the reflexes increases during growth of the first 4–5 nm of MnAs. The orientation of the hexagonal MnAs film was identified as: (1$\bar{1}$00)MnAs‖(110)GaAs and [0001]MnAs‖[001]GaAs.

The surface reconstruction was identified as a (1×2) structure. The distances of the fundamental RHEED streaks in the orthogonal [11$\bar{2}$0]MnAs and [0001]MnAs azimuths correspond to a surface unit mesh with the lattice parameters of 5.7±0.1 Å and 3.8±0.1 Å respectively. This epitaxial orientation, schematically represented in Fig. 1(c), was also confirmed by using asymmetric reflections in XRD measurements at RT. Thus, the (1$\bar{1}$00) side facet of the hexagonal α-MnAs prism is parallel to the GaAs(110) surface with its c-axis parallel to GaAs[001]. By comparing the distances between corresponding GaAs(001) planes (5.65 Å) and MnAs(0002) planes (2.86 Å) an approximate factor of 2 along the GaAs[$\bar{1}$10] (or the MnAs[11$\bar{2}$0]) direction is determined, which should facilitate the epitaxial growth. Indeed, high resolution transmission electron microscopy (HRTEM) demonstrates that this small lattice misfit is accommodated by expanding the MnAs(0002) planes such that they perfectly match with the GaAs(002) planes to form a coherent interface.[18] The lattice misfit along the other in-plane direction (perpendicular to the c axis of the MnAs), defined as $f=d_{\mathrm{MnAs}}\{11\bar{2}0\}-d_{\mathrm{GaAs}}\{\bar{1}10\}/d_{\mathrm{GaAs}}\{\bar{1}10\}$ [where $d_{\mathrm{MnAs}}\{hklm\}$ and $d_{\mathrm{GaAs}}\{hkl\}$ are the distances between corresponding lattice planes] is about 5%. This lattice mismatch is compensated by the generation of regularly arranged localized misfit dislocations.[18]

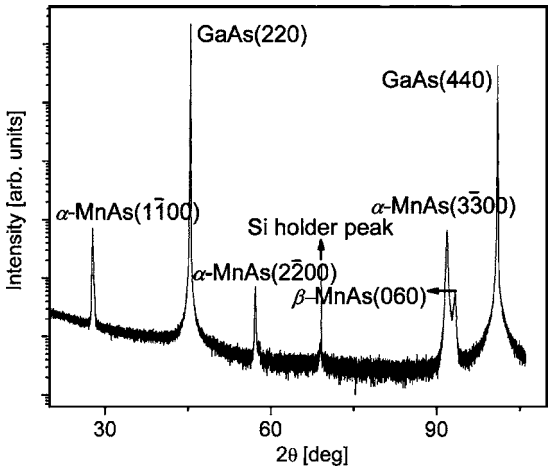

FIG. 2. X-ray diffraction curve (ω-2θ scan) of a 115 nm thick MnAs film on GaAs(110). The α- and β-MnAs peaks are denoted.

Figure 2 presents a symmetric ω-2θ XRD scan of a sample grown on GaAs(110) with a MnAs thickness of 115 nm. Apart from the (220) and (440) GaAs (at 45° and 101°, respectively) and the (1$\bar{1}$00), (2$\bar{2}$00), and (3$\bar{3}$00)α-MnAs peaks (at 30°, 56°, and 91°) also the (060)β-MnAs peak can be clearly distinguished at 93°. The (020) and (040)β-MnAs peaks cannot be resolved since they nearly coincide with the α-MnAs peaks. The presence of the (060)β-MnAs peak is a clear evidence for the coexistence of the two MnAs phases at RT. By recording rocking curves, the peaks belonging to the α-MnAs and β-MnAs phases were independently resolved and the comparison of the integrated areas revealed that the fraction of β-MnAs ranges between 15% and 22%.

The surface topography of two 115 and 66 nm thick MnAs films imaged by AFM is shown in Figs. 3(a) and 3(b), respectively. The main contrast revealed consists of an array of alternating grooves and ridges oriented along the Mn[0001] direction. This structure is related to the strain mediated coexistence of two phases in the heteroepitaxial film as described in recent studies.[9–11] This conclusion is confirmed by the XRD data in Fig. 2 showing clearly both the α-MnAs phase and the β-MnAs phase. The stripe pattern image, deriving from the two MnAs phases, appears for films thicker than 30 nm with alternating grooves (dark stripes) and ridges (light stripes) showing a remarkable regularity. The periodicity and, consequently, the width of the stripes depend on the thickness of the MnAs film [Fig. 3(c)], while the height modulation ranges from 5 to 25 Å. The ridges in

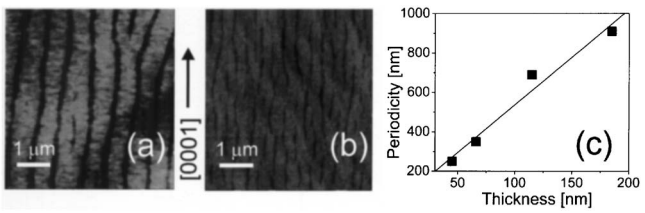

FIG. 3. (a), (b) AFM images of 115 and 66 nm thick MnAs films on GaAs(110). The images show ridges and grooves due to the coexistence of α- and β-MnAs. Image size: 5 μm×5 μm; (c) dependence of the stripe periodicity on the thickness of the MnAs films.

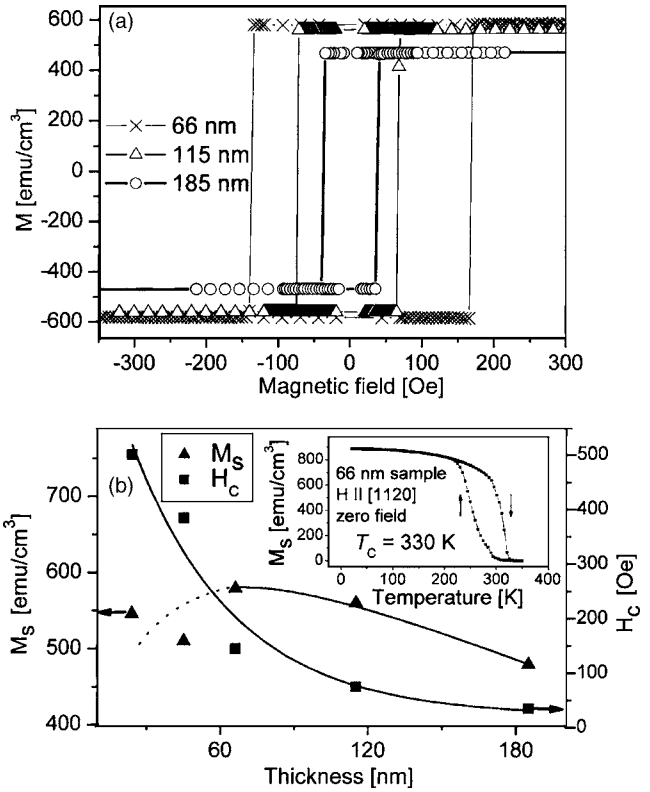

FIG. 4. (a) Hysteresis loops at low fields measured for MnAs/GaAs(110) films of different thickness at RT, with H$\|[11\bar{2}0]$MnAs; (b) coercive field H_C and saturation magnetization M_S as a function of film thickness obtained from the hysteresis loops measured at RT. The inset shows the magnetization as a function of the temperature for the 66 nm sample. The arrows indicate the cooling and heating of the sample during the measurement. Lines are guides to the eyes.

these structures consist of α-MnAs, since it has the larger lattice constant perpendicular to the film, while the grooves consist of β-MnAs.

Figure 4(a) shows SQUID magnetometry measurements for samples of different thickness, which were performed with the external field applied along the $[11\bar{2}0]$ direction, which is identified to be the easy axis of magnetization, whereas the hard magnetization axis runs along the [0001] direction. The magnetization M hysteresis loops measured at RT show a perfect square form, which is observed for all grown samples, regardless of thickness. This behavior demonstrates a significant difference to the MnAs films grown on other GaAs substrate orientations.[11] A T_C value of 330 K was determined, as demonstrated by the temperature dependent magnetization measurement shown in the inset of Fig. 4(b), measured in zero magnetic field. The increasing film thickness affects the coercive field H_c and the saturation magnetization M_S of the MnAs films as shown in Fig. 4(b). The investigated samples show remanent magnetizations from 480 to 580 emu/cm^3 and coercive fields from 35 to 500 Oe. By applying the magnetic field along MnAs[0001] a completely different behavior is observed, where an increase of the magnetic field with a factor of 100 is required to align all magnetic moments parallel to the external field. This demonstrates the high structural quality, concerning crystalline phases and epitaxial orientation of the grown films. The effective anisotropy constant K_{eff}, which is given by $K_{\text{eff}} = \int_0^{M_S} \mu_0 H dm$ amounts to 600×10^3 J/m^{-3}.

In conclusion, epitaxial MnAs was successfully grown on GaAs(110) substrates. The MnAs films grow $(1\bar{1}00)$-oriented with $(1\bar{1}00)$MnAs$\|$(110)GaAs and [0001]MnAs$\|$[001]GaAs. The films consist of the ferromagnetic α-MnAs and the paramagnetic β-MnAs phase, which form a characteristic stripe pattern. All samples possess excellent magnetic properties with perfect square hysteresis loops and a T_C value of 330 K. The coercive fields and the saturation magnetization strongly depend on the film thickness. A large uniaxial magnetic anisotropy of the MnAs films was observed as a consequence of the high crystalline anisotropy. The above observations demonstrate the potential of combining MnAs with the, in terms of spin relaxation, favorable GaAs(110) surface in light emitting diode (LED) structures for spin injection experiments.

The authors are grateful to M. Höricke and R. Hey for the growth of GaAs(110) templates.

[1] G. A. Prinz, Phys. Today **48**, 58 (1995).
[2] K. H. Ploog, J. Appl. Phys. **91**, 7256 (2002).
[3] M. Tanaka, J. P. Harbison, M. C. Park, Y. S. Park, T. Shin, and G. M. Rothberg, J. Appl. Phys. **76**, 6278 (1994).
[4] M. Tanaka, J. P. Harbison, and G. M. Rothberg, J. Cryst. Growth **150**, 1132 (1995).
[5] F. Schippan, A. Trampert, L. Däweritz, K. H. Ploog, B. Dennis, K.-U. Neumann, and K. R. A. Ziebeck, J. Cryst. Growth **201/202**, 674 (1999).
[6] M. Tanaka, K. Saito, and T. Nishinaga, Appl. Phys. Lett. **74**, 64 (1999).
[7] M. Kästner, L. Däweritz, and K. H. Ploog, Surf. Sci. **511**, 387 (2002).
[8] L. Däweritz, M. Kästner, T. Hesjedal, T. Plake, B. Jeninchen, and K. H. Ploog, J. Cryst. Growth **251**, 297 (2003).
[9] V. M. Kaganer, B. Jeninchen, F. Schippan, W. Braun, L. Däweritz, and K. H. Ploog, Phys. Rev. Lett. **85**, 341 (2000).
[10] M. Kästner, C. Herrmann, L. Däweritz, and K. H. Ploog, J. Appl. Phys. **92**, 5711 (2002).
[11] L. Däweritz, L. Wan, B. Jeninchen, C. Herrmann, J. Mohanty, A. Trampert, and K. H. Ploog, J. Appl. Phys. **96**, 5056 (2004).
[12] M. Ramsteiner, H. Y. Hao, A. Kawaharazuka, H. J. Zhu, M. Kästner, R. Hey, L. Däweritz, H. T. Grahn, and K. H. Ploog, Phys. Rev. B **66**, 081304 (2002).
[13] A. Tackeuchi, Y. Nishikawa, and O. Wada, Appl. Phys. Lett. **68**, 797 (1996).
[14] Y. Ohno, R. Terauchi, T. Adachi, F. Matsukura, and H. Ohno, Phys. Rev. Lett. **83**, 4196 (1999).
[15] T. Adachi, Y. Ohno, F. Matsukura, and H. Ohno, Physica E (Amsterdam) **10**, 36 (2001).
[16] T. B. Massalski, H. Okamoto, P. R. Subramanian, and L. Kacprzak, *Binary Alloy Phase Diagrams*, 2nd ed. (American Society of Metals, Metals Park, OH, 1990), Vol. 293, p. 293.
[17] A. Kahn, E. So, P. Mark, C. B. Duke, and R. J. Meyer, Surf. Sci. **71**, 387 (1978).
[18] A. Trampert (private communication).